

## INTEGRATION OF SIS MIXERS, SUPERCONDUCTING LOCAL OSCILLATORS AND OTHER ELEMENTS INTO RECEIVER CHIPS FOR 100–700 GHz

A.N. Vystavkin, V.Yu. Belitsky, V.K. Kaplunenko, V.P. Koshelets,  
S.A. Kovtonyuk, G.V. Prokopenko, A.V. Shchukin, S.V. Shitov,  
M.A. Tarasov

*Institute for Radio Engineering and Electronics  
of the Russian Academy of Sciences  
Mochovaya str. 11, Moscow 103907, RUSSIA  
Fax (7 095) 203 84 14*

### 1. INTRODUCTION

The recent progress in development of high-sensitive SIS mixers of 100–500 GHz frequency region with corresponding noise temperature 30–300 K (Fig.1) [1,2], superconducting local oscillators in this portion of spectrum [3,4] with line-width of the order of 0.7 MHz, SQUID amplifiers of IF signals in 0.1–0.4 GHz region with noise temperature less than 1 K [5], different types of planar antennas, matching elements, filters and so on in integrated implementation and combining them into integrated structures of different complexity [6] clears the way to integrated receiving chips of mentioned frequency region. Receivers based on integrated chips comprising mentioned superconducting elements will be comparatively inexpensive, having small dimensions and weight and necessary reliability. Fabrication of such compact receiving chips opens the way to the creation of superconducting matrix for image receiver.

Results of corresponding investigations, developments and estimations of creation of entirely superconducting integrated receivers for frequencies up to 700 GHz are given. Results not published earlier are given in more details.

### 2. JUNCTIONS FABRICATION TECHNOLOGY AND LAYOUT DESIGN

Our technology group has the possibilities to fabricate all types of superconductive circuits that are designed and investigated in our laboratory. These possibilities based on high quality Nb–AlO<sub>x</sub>–Nb tunnel junction fabrication process which has been described previously [7,8]. In this process we use stress-free Nb films for three-layer sputtering and well-known "self aligned" process for junction geometry determination.

The junctions properties (specific capacitance, magnetic penetration depth in the Nb films) have been investigated in wide range of critical current densities [8]. The results obtained make possible to design and fabricate complex microwave receiving and Single Flux Quantum (SFQ) circuits perfectly matched in the desired frequency range.

For fabrication of SIS arrays consisting of numerous identical high critical current density Nb–AlO<sub>x</sub>–Nb junctions we utilize usual optical lithography and double step "self align" process (cross method). Here we provide usual "self align" operational procedure: lithography, RIE, anodization,

insulator deposition (SiO) and lift-off twice, defining two comparatively long ( $1.5 \times 10^4 \mu\text{m}$ ) junctions perpendicularly each other. The square junction with approximately  $1 \mu\text{m}$  dimensions (decreasing dimensions is due to RIE underetching) are realized on the crossing. In our RIE setup it is possible to keep underetching at  $0.4 - 0.7 \mu\text{m}$  and fabricate submicrometer Nb-AlOx-Nb tunnel junctions in controllable manner.

In our laboratory a CAD system for photomask constructing was developed. It consists of different kind calculation and superconductive circuits modeling software which is specified for digital RSFQ logic and SIS mixer circuits. Based on this modeling photomasks are plotted using PC based drawing systems. Special program provides analyzing of the particular topology and converts drawing data to data convenient for an E-beam photomask processing machine. The program comprises drawing data converting module, topology analyzer (arbitrary topology), and data proceeding module which is accommodated for the concrete photomask processing machine. Thus all lines from the primary drawing of the future chip ready for producing photomasks is CAD supported. Now we are using this technology for all our investigations.

### 3. SERIES RF / PARALLEL IF ARRAYS OF SIS JUNCTIONS FOR WAVEGUIDE MM WAVES MIXERS.

Since 1982 we have developed mixing SIS arrays which have unique design because of parallel connection between the junctions for both dc bias and IF output signal but for rf signal the connection is still in series [9] (SRF/PIF design). The original idea of this connection was appeared as a result of analysis for earlier experiments with SIS mixers which had shown number of problems [10].

This problems have been overcome by using the SRF/PIF design because it provides simultaneously:

- i) low capacitance and high impedance referred to input port which are equivalent to those of series array;
- ii) the same optimum voltage for all junctions in the array which is feature of an ideal array;
- iii) tuning out intrinsic capacitance by means of special design of bias circuits;
- iiii) low output impedance close to  $50\Omega$  without using any transformers.

Simple relationships can be established to calculate optimum number  $N$  and parameters of single junctions in the array as well. The SRF/PIF connection provides for the mixing array *increased input* impedance  $NG_{\omega\omega}^{-1}$  seen by *rf* source and *decreased output* impedance  $G_{00}^{-1}/N$  seen by IF amplifier. Here  $G_{\omega\omega}^{-1}$  and  $G_{00}^{-1}$  are input and output impedances of pumped single junction respectively [11]. The optimum number  $N$  of junctions in such array could be calculated to get *desired* both input and output impedances in followed manner [12]:

$$N^2 = (G_1/G_s)(G_{\omega\omega}/G_{00})$$

Here  $G_s$  and  $G_1$  are real parts of *rf* source and IF load admit-

tances need to be matched respectively. The ratio  $G_{\omega\omega}/G_{\infty\infty}$  could be obtained from experimental junction IVC using numerical calculations based on three-port model [11].

The integrated bias circuits can be used not only as an *rf* isolation, but also as tuning elements to tune out junction's intrinsic capacitance. Fig.2 illustrates the design principle have been developed for the new arrays. It shows the transition from purely resistive nonlinear elements connected in series by mean of assembling with lumped resonant circuits toward tuned arrays with series *rf*/parallel IF connection of SIS junctions (crosses). The figures a)-c) presents the way to combine together even number of junctions. The base unit is the original two-junctions cell with three electrodes and *rf* rejection filter  $L_i C_i$  (see Fig. 2).

Two different ways could be used to tune odd number array. The examples d)-f) and g)-i) illustrate this difference which is mainly in parameters of tuning inductances and capacitances. In the case f) tuning capacitances should be equal to junction capacitance  $C$ , but for case i) only half of that. The ratio for inductances should be inverse. The tuning bandwidth is wider for the case i) if junctions parameters are kept the same.

The treatment above allows to state that one could obtain perfect matching condition for SIS mixing element without any input/output transformers if mentioned requirements are satisfied.

In Figure 3 the layout of experimental five-junction array is shown. It is an example of practical realization of variant i) from Figure 2. The tuning inductances are patterned as short circuited two wire lines. It should be noted that capacitance coupled to the tuning inductance is approximately *four* times less than for individually tuned junction. It makes easier to design inductive elements for higher frequencies, because the loop need become not too small.

Laboratory tests of the experimental receivers were carried out in liquid helium cryostat at mixer ambient temperature in range 4.2-5 K. The input signals were obtained from matched loads at 80K and 300K placed in front of the horn antenna on the top of the cryostat. The mixers have only one tuning element (backshort plunger) which can operates as an image rejecter. The output IF signal centered at 1.5 GHz was amplified by cold low-noise ( $\leq 10K$ ) IF amplifiers and registered by spectrum analyzer.

The magnetic field up to 6000 A/m could be applied to the mixing array by superconducting coil, but it was not really used because the new arrays have suppressed critical current. The suppression is caused by weak random magnetic fields coupled to the tuning loops which are galvanically connected to the pair of junctions (see Fig.2). This configuration is very similar to *dc*-SQUID which has critical current very sensitive to magnetic field. This property is very helpful to suppress Josephson steps in sub-mm region.

The receiver noise temperature measurements have been carried out by using data acquisition system. This system is based on the AT-286 IBM compatible computer and HP8566 spect-

rum analyzer connected together by GP-IB interface. The program was written in C language and performs digital processing and graphics based on the data obtained from spectrum analyzer. It makes experiments more convenient and accurate. All variants presented in Figure 2 have been tested as mixing elements. The low-noise wide band receiver performance has been obtained even if very simple input and output circuitry was used (i.e. full height input waveguide and single tuner; absence of any output transformer).

In spite of similar results were obtained with 2, 4 and 5-junctions arrays in 2 mm band (5, 10 and 11-junctions array in 3 mm band [13]) it was found that arrays which parameters better fit the *optimum matching conception* demonstrated wider tuning range and lower noise temperatures.

In Figure 4 the summary for the best receivers tested in 40-150GHz frequency range is presented in comparison with quantum limit  $hf/k$ . This data have been obtained with parallel biased arrays as a receiver front end mixing elements.

The *optimum matching conception* have been developed for SIS array mixers and was successfully confirmed in frequency range 40-180 GHz. This conception could be applied for full height waveguide mixers and for mixers integrated with strip-line structures as well. Very low noise parameters ( $T_r \leq 50K$ ) were demonstrated in 40-150 GHz frequency region.

#### 4. QUASIOPTICAL SIS MIXERS WITH MICROSTRIP TRANSFORMERS AND SPIRAL ANTENNAS

Another approach is associated with open structure SIS mixers based on equiangular spiral antenna with integrated on chip coupling circuitry and a single or pair stacked SIS junctions. Open structure SIS mixers are under developing in our laboratory since 1984. From the very beginning the equiangular spiral antenna was used. The first design was specified to use Si substrate placed in oversized circular waveguide at 75 GHz. Inductive loop with DC block capacitor was integrated in the antenna apex area for SIS junction capacitance compensation at 75 GHz.

Next step in the integration circuit was made in 1989: it was suggested to connect SIS junction and antenna via a microstrip impedance transformer with length little bit longer than quarter of wavelength. This additional piece of microstrip line acts as inductance for resonating out the SIS junction capacitance. Quarter wavelength microstrip transformer is used for transformation of already real impedance to spiral antenna driving impedance  $\sim 44$  Ohm [14] and later was successfully applied to 115 GHz spiral antenna SIS mixer, Fig.5 shows the topology of the 115 GHz receiver chip [15].

Further developing of this technique is associated with twin SIS junctions compensation circuit which was suggested [16] to use for resonating out SIS junctions capacitance by mean conjugating of the impedance of one to compensate reactance of another. The twin junctions compensation circuit in combination with microstrip impedance transformer was

implemented for 500 GHz SIS mixer receiver.

The result which is presented at the present conference [2] was obtained in a very close collaboration with Chalmers University of Technology with a group of Prof. E. Kollberg. The receiver demonstrated noise temperature below 300 K DSB at the frequency band 450–515 GHz. Relatively large optically lithographed SIS junctions and the particular topology of the twin circuit make very easy suppression of the Josephson steps on pumped IV curve. Low normal state resistance of the junctions using both in impedance transformer and twin circuits improve saturation power of the SIS mixer. Our calculations show very good prospects of the integrated structure based on open structure SIS mixer and twin junctions tuning circuit for submm band applications up to 800–900 GHz.

## 5. SIS ARRAYS INTEGRATED WITH MATCHING ELEMENTS AND PLANAR ANTENNAS

Integration of SIS junction arrays with planar wide band antenna allows to increase instantaneous bandwidth of receiver up to octave in comparison with rather narrow-band traditional waveguide mixers with SIS junction arrays or planar antennas with integrated single microstrip transformer and single SIS junction. Integrated receiving structure comprising self-Babinet-complementary spiral antenna, array of SIS junctions connected in series as seen by the RF but are parallel DC-biased through the same inductances that provide the tuning for the SIS junctions capacitance has been designed and experimentally studied. Array was designed for 80–160 GHz wave band and consists of 5 SIS junctions  $1.5 \mu\text{m}^2$  area each, six inductive short-ended slot-lines and two decoupling capacitances. Effective direct detector bandwidth of such structure with quantum efficiency equals unity has been estimated as wide as 70 GHz. Noise temperature of heterodyne mixer has been measured in three-lens Gaussian beamguide by means of hot/cold loads method, yielding receiver DSB noise temperature 80 K. IF mixer port load bandwidth and thermal background radiation influence on IV curve and saturation of SIS mixer have been studied.

The waveguide type SIS mixers signal frequency increasing over achieved values  $\sim 500$  GHz [17] is connected with increasing problems of mechanical elements fabrication tolerances and increasing with frequency losses in waveguides and plungers. From radioastronomy point of view it is much easier to use quasioptical methods of focusing and transmission of initial signal which is presented at the output of radio telescope as a gaussian beam.

The combining quasioptical beamguide and wide bandwidth planar antenna allows to design more broadband device than waveguide type receiver system having conversion gain and noise temperature close to the best achieved in waveguide type mixers [18]. Among disadvantages of quasioptical systems may be mentioned the absence of tuning elements and possibility of antenna-substrate interaction, which can lead to beam pattern distortion at some frequencies.

Advantages and drawbacks of both mentioned methods leads to conclusion about combining series-parallel arrays and integrated planar antennas in order to obtain effective mixer matching in wide bandwidth and increasing of central frequency up to 700 GHz and higher. Problems of external broadband thermal radiation on mixer parameters and its saturation in such system should be carefully studied.

In these experiments we used equiangular self-Babinet two-arm spiral antenna similar to [18] with shape according to relation  $r=R_0 \exp(a\phi)$  where  $r$  and  $\phi$  - polar coordinates,  $a$  and  $R_0$  - constants (see Fig. 6a). Value of  $a=0.36$  was chosen as compromise between two cases of wider beam pattern with lower and more elliptical beam pattern with higher values. Impedance of such antenna placed on quartz hyperhemisphere corresponds to relation  $Z_{ant} = Z_0 / (0.5 + 0.5n^2)^{1/2} \approx 114 \Omega$  in more than decade frequency band.

SIS junction array (Fig. 6b) consists of five junctions. Six sections of end-shortened slot lines were used for parallel connection of junctions and capacitances tuning out. The central sections are  $140 \mu\text{m}$  long and outer sections are  $70 \mu\text{m}$  long. Area of each junction is  $1.5 \mu\text{m}^2$  and the whole structure designed for central frequency 115 GHz is equivalent to single junction of  $0.3 \mu\text{m}^2$  area.

Such integrated circuit operates without additional choke filters in IF channel preventing signal leakage because spiral antenna itself has a useful property of automatic currents cutoff which means that only central part of antenna takes part in signal receiving. The length of such active part of antenna not exceeds the signal wavelength, i.e. 2-3 mm in our case.

In order to make direct measurements of antenna beam pattern and to adjust precisely 3-lens beamguide at room temperature we have fabricated similar structures with golden antenna of the same shape and bismuth microbolometer instead of SIS array. Bolometers were made of Bi film 200 nm thick,  $30 \Omega/\square$  resistance,  $3 \mu\text{m}$  width and 9-16  $\mu\text{m}$  length. Beam patterns of bare antenna on quartz substrate, the same on quartz hyperhemisphere lens and also with counterreflector behind antenna are shown in Fig. 7. Data presented in Fig. 7 are normalized to maximal signal corresponding to the last case.

In IF channel the cold amplifier and circulator were used to prevent standing waves at the output of the mixer. Such amplifier was matched with SIS array in bandwidth over 0.5 GHz. It may lead to the mixer output saturation. For mixer dynamic range increase it is desirable to make IF band narrower and short-circuit its output out of this band. For this purpose we have tested two types of filters. First consists of microstrip line section and decoupling capacitor, and the second - of antenna+leads inductance and capacitor comprising together series resonant circuit.

Matching efficiency at IF was estimated from IF port noise temperature, measured with SIS junction shot noise as noise source. In general current noise in SIS junction cor-

responds to the relation  $I_N^2 = 2eI \cdot \Delta f \cdot \coth(eV/4kT)$  which is reduced to simple shot noise relation  $I_N^2 = 2eI \cdot \Delta f$  for voltages above the energy gap. Noise temperature of the receiver was measured in DSB mode with hot (300 K) / cold (80 K) loads. In this experiments a sufficient influence of hot/cold switching on IV curve and IF noise was observed even in the absence of LO power for array with dc resistance 20  $\Omega$ . This fact is clear illustration of mixer input saturation by broadband thermal radiation of the order of 100 GHz with effective temperature 300 K. Observed in the same experiment rather high noise temperature equals to 180 K at 108 GHz is due to this saturation effect.

Another SIS array with 10  $\Omega$  normal resistance was tested with switching on and off additional cold attenuator with losses 3.8 dB. The receiver noise temperature with open attenuator was 350 K, and with closed attenuator 200 K. For another cold attenuator with 8.8 dB losses the receiver noise temperature was 250 K and 80 K for open and close cases correspondingly, see Fig.7b. These experiments show that the main problem for such very broadband SIS mixers is the output saturation and it may be solved by restricting input and output bandwidths.

## 6. SUPERCONDUCTING MILLIMETER WAVE RECEIVER INTEGRATED ON A CHIP

At frequencies above approximately 300GHz a problem of local oscillator for spectral receivers arises; it is especially important for satellite receivers and/or image receivers combined many mixers. This is why the idea of using superconducting local oscillators integrated with SIS mixers looks very attractive.

Josephson oscillations in long tunnel junctions due to solitons' motion along the tunnel region can be used as a microwave source. The frequency of oscillation  $f$  is dependent on the dc voltage  $V$  across the junction according to the Josephson relation:

$$f = 2eV/h$$

The soliton mode generation has very narrow linewidths [19] and the frequency is strictly determined by the junction length due to resonant properties of the junction cavity [20]. Moreover it is very difficult to obtain microwave oscillations at frequencies higher than approximately 150 GHz in the "soliton" mode. The flux-flow mode of oscillation (FFO) in the similar long junction uses viscous motion of the solitons (see, for ex. [21]) and can be tuned almost permanently up to 500 GHz with large output power. The experimental integrated receiving structure comprises SIS array mixer integrated with Flux-Flow type Josephson oscillator used as a LO source on the same substrate. The mixer was designed based on the new SRF/PIF conception (see section 3). The FFO local oscillators and SIS array mixing elements have been sputtered in the same run onto a 15x24x0.1 mm quartz substrate which then was cut down to chips of 0.5x5.3x0.1 mm size (the same size as ordinary mixing chips).

The Nb-AlO<sub>x</sub>-Nb trilayer process has been used [22] to form both generating and receiving junctions, so they have the same current density.

An equivalent circuit for the experimental structure is presented in Fig.8. It is simplified version to clarify the actual layout shown in Fig.9. Bottom electrode (1) of the structure serves as a ground plane for impedance transformer (7) and was shaped as low-pass filter to prevent leakage of microwave power along the substrate. The 5-step octave bandwidth microstrip impedance transformer with ratio 1:30 is loaded by a Ti film resistor (8) to avoid reflections and resonances in the LO part. The transition from transformer to coupling probes (9) provides isolation for the input rf signal and about -10 dB attenuation for the LO power delivered by the FFO. The 10 μm gap between probes serves as a dc-block. The substrate could be split along this gap to obtain two independent elements: FFO and mixing SIS array.

The experimental mixing section was based on two junctions array [19]. The array have an inductive tuner designed to tune out the reactance of both junctions around 150 GHz (see Fig.2a in section 3). The top electrode (3) forms a low-pass filter for the output IF signal. This filter design is based on quarter-wave coplanar and microstrip lines. The new receiving structure has to be used with three independently dc control current sources. One more source is needed to produce a magnetic field to control the FFO junction. The magnetic field was applied to the chip by a superconducting coil in the plane of the junction. The field up to only 4-8 A/m was used to provide the tuning of FFO.

The integrated receiver has been tested in the same mixer block which was used for ordinary mixing experiments. The mixing block has full height rectangular waveguide (0.8x1.6 mm) and single tuning backshort of circular shape. The input noise signal has been supplied to the mixer through a oversized waveguide. The LO power from BWO and Gunn oscillator have been introduced by means of a cold diplexer (-26 dB) mounted on the mixer block input flange.

The IF output signal (1.3-1.8 GHz) passed through cooled isolator was amplified by cooled FET amplifier. Typical noise temperature of the IF channel estimated from the SIS junction shot noise was less than 10 K.

The maximum power 80 nW coupled to the array have been estimated at a FFO frequency range 100-140GHz. It corresponds to a normalized rf voltage equal to  $\alpha \approx 1$  that is sufficient to pump the SIS array mixer. However the minimum receiver noise temperatures (67K at 133 GHz and 85 K at 140 GHz) were obtained with lower powers ( $\approx 20$ nW).

The LO power coupled to the array changes when the backshort is moving. It is very similar to the case when external LO used. The experimental data for two different chips (#1 and #2) tested in two different laboratories in comparison with two different external LO (BWO and Gunn oscillator) are presented in Fig.10. It is surprising that the receiver noise temperatures obtained with the FFO could be somewhat lower at certain frequencies than for the case of mixer pumped by external oscillators.



It was demonstrated experimentally that a Flux-Flow LO can provide good stable and repeatable low-noise operation of a SIS receiver at short millimeter wavelengths.

## 7. FLUX FLOW OSCILLATORS STUDIES

Superconducting Flux-Flow Oscillators (FFO) integrated on the same chip with microwave detector have been experimentally investigated in the wide frequency range 100 - 450 GHz. A possibility to adjust the oscillator rf power by changing the bias current and /or magnetic field has been demonstrated. The detected microwave power as high as  $0.3 \mu\text{W}$  has been achieved at FFO frequency 375 GHz. The linewidth of the FFO about 1 MHz has been estimated from different mixing experiments. An integrated circuit which consists of a FFO, coupling transformer sections, superconducting high frequency attenuator and microwave detector with tuned out capacitance have been designed and successfully tested.

The possibility to create a SIS receiver with integrated Flux-Flow Oscillator (FFO) has been recently demonstrated [3,4]. The frequency tuning in the range 280 - 330 GHz with linewidth 2.1 MHz have been reported in [4]; the front-end noise temperature of real integrated receiver as low as 85 K at 140 GHz has been achieved [3]. In this report we present the results of farther investigation of FFO and more complicated integrated circuits. High quality Nb-AlOx-Nb junctions ( $j_c \approx 10^3 \text{ A/cm}^2$ ) were used as elements of the integrated circuits; technological procedure for their fabrication was published in [3,23].

A first type of the integrated circuit consists of a long Josephson junction, a coupling impedance transformer section and a microwave detector with tuned out capacitance; it is similar to described in [3]. To provide the additional dumping the long Josephson junction was shunted by low inductance  $M_0$  resistor ( $R_n < R_s < R_j$ ). Nevertheless even for large external magnetic field together with a flux-flow step (FFS) the weak Fiske steps (FS) at  $V_{FS} = n\Phi_0 v / 2L$  occurred ( $v$  - is Swihart velocity,  $L$  - junction length). At changing of the magnetic field  $H$  the flux-flow step moves on IVC:  $V_{FF} = v\Lambda\mu_0 H$ , where  $\Lambda$  - magnetic thickness of the junction.

Flux-flow step "emphasizes" the corresponding FSs and increases their amplitude. Therefore it was possible to realize flux-flow regime at appropriate FS providing the small dynamic resistance and permanency of the generated frequency.

Fig. 11 shows the IVC of the detector for different FFO bias currents at constant magnetic field. One can see that the frequency ( $f \approx 375 \text{ GHz}$ ) is fixed and only changing of the power takes place. It should be noted that for the same  $H$  but at different bias currents the generation of 175, 375 and 450 GHz was observed. The same was also possible at constant bias current by changing the magnetic field only to provide the variation of the FFO power (similar to shown in Fig. 11) without distinguished changing of the FFO frequency.

For measuring the FFO linewidth the integrated receiver

circuits [3] have been used. The signal from external synchronized generator,  $f = 70$  or  $140$  GHz (4-th or 8-th harmonic of the  $15 - 22$  GHz pure linewidth source) was mixed with  $140$  GHz FFO signals in SIS junctions array. The output signal was connected to room temperature  $1.5$  GHz IF amplifier. One of the measured spectrum is shown in Fig. 12, it's possible to estimate the 3 dB linewidth which is about  $0.7$  MHz. Theoretical estimation of the linewidth [24]

$$\delta f = (\pi kT / \Phi_0) \cdot (R_d^2 / R_{dc})$$

gives a smaller value about  $100$  kHz. It should be mentioned that as a rule some additional modulation of the FFO signal took place. This effect was observed in quite different set-ups and probably is connected with the small instabilities of fluxon motion in long Josephson junction.

To achieve the ultimate parameters of a SIS mixer the local oscillator (LO) power should be carefully controlled without any changing of the FFO frequency. We have designed and investigated integrated circuits which comprise FFO, microwave detector, matching elements and adjustable superconducting high frequency attenuator. The action of this attenuator is based on the change of the microwave impedance at variation of the SIS junction bias. Fig. 13 shows the action of the integrated attenuator at frequency  $325$  GHz. Because of non optimal design there was a large enough attenuation even in open state; numerical calculations predict that the performance of the integrated attenuator circuit could be considerably improved.

## 8. SIS ATTENUATOR FOR FFO OSCILLATOR

To achieve the optimal performance of the SIS mixer the LO pumping level should be adjusted with the accuracy about  $1$  dB. It's especially important for synchronous arrays of the Josephson junctions, whereas for Flux Flow Oscillators (FFO) microwave power could be tuned within large enough range by changing the current bias and/or magnetic field. But even for FFO the adjustment of the power might result in changing frequency and/or linewidth. To provide the possibility of fine tuning of the microwave power we have introduced a new integrated element - superconducting attenuator for high frequency signals.

An action of the attenuator is based on the change of the microwave impedance  $Z$  of a superconducting tunnel junction at variation of its dc voltage bias  $V$ . The microwave impedance  $Z(V)$  is dependent also on the frequency  $f$ , but for  $f < eV_g/h$  one can distinguish three basic regions on IVC of a SIS junction. At  $V \gg V_g$  the real part of the impedance  $\text{Re}Z$  is equal to normal state resistance  $R_n$ ,  $\text{Re}Z \gg R_n$  at  $|V| < (V_g - hf/e)$  and  $\text{Re}Z < R_n$  at  $V \cong V_g$ . To realize this simplified picture the junction critical current should be suppressed and capacitance of the SIS junction has been tuned out. The attenuator junctions could be placed in microstrip line between signal source and detector in series or/and parallel; in both cases

the  $R_n$  should be about characteristic impedance of the line. The attenuator is closed at  $|V| < (V_g - hf/e)$  for series connection and  $V \cong V_g$  for parallel one; the "open" state takes place at opposite combination of the biasing. Numerical calculations, based on Tucker's theory, have confirmed this consideration.

The different types of the integrated microcircuits have been designed and realized to check the idea of impedance attenuator. An equivalent diagram for one of the integrated circuit is shown in Fig. 14. The 70 GHz microwave signal was introduced in the circuit through fin-line antenna and microstrip quarter wave transformer. An attenuator itself consist of three identical sections  $-S_1, S_2, P$ . Each sections combines two SIS junctions ( $A=25 \mu\text{m}^2$ ,  $R_n=4-8 \Omega$ ), which are connected in series for RF signals but in parallel for DC; the capacitance of the junctions are tuned out at signal frequency by small inductance. Two series attenuator sections  $S_1$  and  $S_2$  are connected together by large inductance  $L$ . After attenuator the microwave power through transformer  $T_2$  was connected to the detector SIS junction ( $A=5 \mu\text{m}^2$ ,  $R_n=20 \Omega$ ); its capacitance is tuned out by inductance of the microstrip stub.

All microcircuits which include three superconducting Nb layers and two double  $\text{SiO}_2$  layers have been fabricated using technological procedure developed for SIS and RSFQ devices (Section 2). High quality Nb-AlO<sub>x</sub>-Nb junctions with critical current density  $j_c \cong 2 \cdot 10^3 \text{ A/cm}^2$  and subgap to normal state resistance ratio  $R_j/R_n > 20$  were used as attenuators and detectors.

Fig.15 demonstrates the action of the series attenuator (S-att) at  $f = 74.6 \text{ GHz}$ ; the IVC of the S-att, measured between terminals "1" and "3", is presented in the insertion. The IVCs of the detector junction were obtained at four different bias voltages on the S-att, these voltages are marked in the insertion also. One can see the significant changing of the detected microwave power at variations of S-att bias. At point "1" ( $V \cong V_g$ ) the S-att is open ( $\alpha \cong eV_{rf}/hf \cong 2$ ) while at point "4" ( $V \cong 0$ ,  $\alpha \tau \approx 0.02$ ) IVC of the detector is close enough to the autonomous one which is shown by dashed line in Fig.15. So, it's possible to introduce the attenuation of the microwave power at least 17 dB by changing the bias of the S-att.

To investigate the dependence of the attenuation on bias voltage more carefully we have applied to the circuit modulated microwave power and measured by lock-in amplifier the response of the detector. The qualitative agreement with the numerical calculations has been found. The detailed experimental results and their comparison with the theory will be published elsewhere.

The presented results have confirmed the possibility to

create an adjustable superconducting attenuator for microwave signals. The wide dynamic range (more than 15 dB) together with small losses in the "open" state have been demonstrated in both numerical calculations and experiments. New elements could be successfully used in integrated mm wave and terahertz receivers as precisely controlled attenuator and microwave modulators.

## 9. IF SQUID AMPLIFIER AND ITS TESTING BY SIS JUNCTION NOISE

The noise and signal parameters of several types of the IF amplifiers based on the different SQUIDs with integrated and hybrid input coils were studied. A new type of the multiloop dc SQUID with integrated input coil and extremely low stray capacitances was designed. The inductance of a four-loop SQUID was 100 pH, the input coil inductance 1.3 nH and mutual inductance 300 pH. The noise temperature of untuned SQUID amplifier with hybrid input coil at 100 MHz was  $1.2 \pm 1$  K and the power gain has exceeded 20 dB. The tuned integrated four-loop amplifier at 450 MHz has nearly 20 dB gain in 60 MHz band. For the noise calibration of such amplifiers we used SIS junctions as a shot noise source or cooled attenuator and a room-temperature semiconductor noise source.

The main disadvantages of the previous studied SQA are relatively low operating frequency and a high influence of external magnetic fields on SQA parameters. For the signal frequency increase with preservation of the low noise temperature and high gain the Josephson frequency in the SQUID loop should be increased and it means that the loop inductance and capacitance should be decreased. In the well-known integrated SQUID structure [25] the stray capacitance in the loop exceeds 10 pF. The capacitance between the evaporated above the loop input coil and the loop is even more and this capacitance leads to the significant stray input-output feedback.

To eliminate these disadvantages and increase the input signal frequency and band we designed a four-loop dc SQUID with an integrated input coil in the form of rectangular turns inside the loops (see Fig.16).

The SQUID loop inductance consists of the four parallel connected square loops of  $200 \times 200 \mu\text{m}^2$  size. The input coil consists of four series connected square turns with Nb film widths  $10 \mu\text{m}$ . Parallel connection of the loops allows to reduce inductance of the loop and increase the resonant frequency. Series connection of the input turns allows to increase the input coil inductance and make easier the impedance matching with the input 50 Ohm line. The position of input turns inside the loops was chosen to reduce stray input-output capacitance.

The SQUID loop inductance in this construction is 100 pH, input coil - 1.3 nH, mutual inductance 300 pH. The stray capacitance in SQUID loop 1.8 pF, the sum junctions capacitance 0.8 pF, input coil capacitance 0.3 pF, loop-coil capacitance 2.2 pF. The Nb-AlO<sub>x</sub>-Nb shunted tunnel junctions of  $2.5 \times 2.5 \mu\text{m}^2$  area were used as Josephson junctions. The input

coil resonant frequency is estimated to be 8 GHz and the loop resonant frequency 10 GHz.

Since the input coil inductance is rather small and its reactive impedance at 300 MHz is  $\sim 2.5$  Ohm, then to match the input 50 Ohm line and the input coil we used the resonant circuit matching [26]. In the design of the matching circuit the sufficient element is series additional inductance  $L_s$ , which was in the range 5–15 nH and depends on the size of connecting leads. Scaling the input circuit elements to the input resonant circuit one may obtain the equivalent capacitance  $C_r \approx C_1 + C_0$  and resistance  $R_r \approx R(C_1/C_0)^2$ . According to [27] the optimal Q-factor is  $Q \approx (1 + L_s/L_i)/\alpha^2$  which in our case gives  $Q_{opt} \approx 10$  and taking into account  $Q \approx \omega L_s/R_r$  one could obtain  $C_1 \approx 0.2C_0$ .

For such matching circuit parameters the dependence of the amplified noise signal on frequency is shown in Fig.17. The measured noise temperature of such SQUID amplifier was  $T_N < 0.5$  K at signal frequency  $f \approx 430$  MHz in 60 MHz frequency band.

The nearest competitor of SQA is cooled HEMT amplifiers which have  $T_N \sim (1-3)$  K at  $f \sim (1-3)$  GHz, but have rather high power dissipation equal to tens milliwatts and nearly achieved their asymptotic parameters. On the other hand SQA has more than one order reserve in the margins of gain, noise temperature and signal frequency even on the basis of the present technology. The sufficient advantages of SQA are extremely low power dissipation of several picowatt, small size  $\sim 1$  mm<sup>2</sup> and full electrical, material and temperature compatibility with the superconducting sensitive devices such as Josephson and SIS mixers.

For these measurements we use SIS junction as calibrated shot noise source. In such configuration the measurements layout is similar to SIS mixer with SQUID IF amplifier and may be useful to combine both of these devices in single chip. The problem is to design and fabricate integrated matching circuit with proper series and parallel capacitors. Direct connection of integrated capacitor to the input coil was unsuccessful because of too low Q-factor of input circuit. Such integrated circuit needs additional series inductance in order to increase Q-factor and to achieve high enough gain and low noise temperature.

#### ACKNOWLEDGEMENTS

Authors would like to acknowledge hospitality, help and many useful discussions to Prof. E.Kollberg, Prof. R.Booth, D-r S.Jacobsson, N.Whyborn, C.-O.Lindstrom from Applied Electron Physics Department of Chalmers University of Technology (Gothenburg, Sweden).

Fruitful discussions with J.Mygind and A. Ustinov are gratefully acknowledged.

This research supported in part by Russian State Scien-

tific Program "HTc Superconductivity" under contracts No 90463, 91009 and by Ministry of Science, Higher education and Technical policy of Russia under order N 580.

## REFERENCES

1. SIS Workshop 11-12 May 1992, Zernice Science Park, Groningen, The Netherlands.
2. V.Yu.Belitsky, et al, 0.5 THz SIS receiver with twin junction tuning circuit, this conference.
3. V.P.Koshelets et al, IEEE Trans on Appl. Supercond. (1993), to be published.
4. Y.M.Zhang, et al, Appl.Phys.Lett., 1993, to be published.
5. M.A.Tarasov, et al, IEEE ASC, v.2, N 2, 1992, 79-83.
6. A.N.Vystavkin, et al, Proc. 22 European Microwave conf., 24-27 Aug. 1992, Helsinki, Finland, v.2, 981-986.
7. An.B. Ermakov, et al, Ext. Abstr.1989 Int. Supercond. Electron. Conf. (ISEC'89), Japan, pp.294-297.
8. V.P.Koshelets, et al, IEEE MAG, v.27, pp 3141-3144.
9. A.N.Vystavkin, et al, Physica 109&110 pp 2064-2066, 1982.
- V.Yu.Belitsky, V.P.Koshelets, G.A.Ovsvyannikov, S.V.Shitov, "RF Detector", a.c. (USSR patent) No. 12708679, 1984.
10. A.R.Kerr and S.-K.Pan, Int. J. IR&MM Waves, v 11, N 10, pp 1169-1187, 1990.
11. J.R.Tucker, M.J.Feldman, Rev. of Mod. Phys., vol. 4, pp 1055-1113, 1985.
12. An.B.Ermakov, et al, IEEE MAG, v. 27, N 2, pp 2642-2645, 1991.
13. S.V.Shitov, et al, Supercond. Sci. Technol., v 4, pp 406-408, 1991.
14. Belitsky V.Yu., et al, Extended Abstracts of ISEC-89, TOKYO, 1989, pp 179-182.
15. Belitsky V.Yu., et al., Int. J. of IR & MM Waves, v.13, no 4, pp. 389-396, 1992.
16. V.Yu. Belitsky and M.A. Tarasov, IEEE Trans. on Magn., vol. MAG-25, 1991.
17. G.De Lange, et. al., Proc. 3 Int. Symp. on Space Terahertz Technol., Ann-Arbor, Michigan, p.16, March 1992.
18. T.H.Buttgenbach, et.al., IEEE MTT, vol.36, p.1720-1725, 1988.
19. An.B.Ermakov, et al, IEEE Trans. on Magn., MAG-27, No.2, pp 2642-2645, 1990.
20. E.Joergensen, et al, Theory and Experiment Phys. Rev. Lett., vol.49, No.15, pp 1093-1096, 1982.
21. T.Nagatsuma, et al, The Trans.IECE of Japan, vol.E-66, No.11, pp 680-681, 1983.
22. V.P.Koshelets, et al, IEEE Trans. on Magn., MAG- 27, No.2, pp 3141-3144, 1990.
23. V.P.Koshelets et al, IEEE Trans on Magn, MAG-27, (1991), 2642.
24. E.Joergensen et al, Phys Rev Lett, 49, (1982), 1093.
25. M.B.Ketchen, J.M. Jaycox, Appl.Phys.Lett. -1982.-40,n8.-P.736-738.
26. T.Takami, et al, IEEE Trans. Magn. -1989.- 25,N 2.-p.1030-1033.
27. C.Hilbert, J.Clarke, J.Low Temp. Phys. -1985. -61,n3/4. -P.263-280.

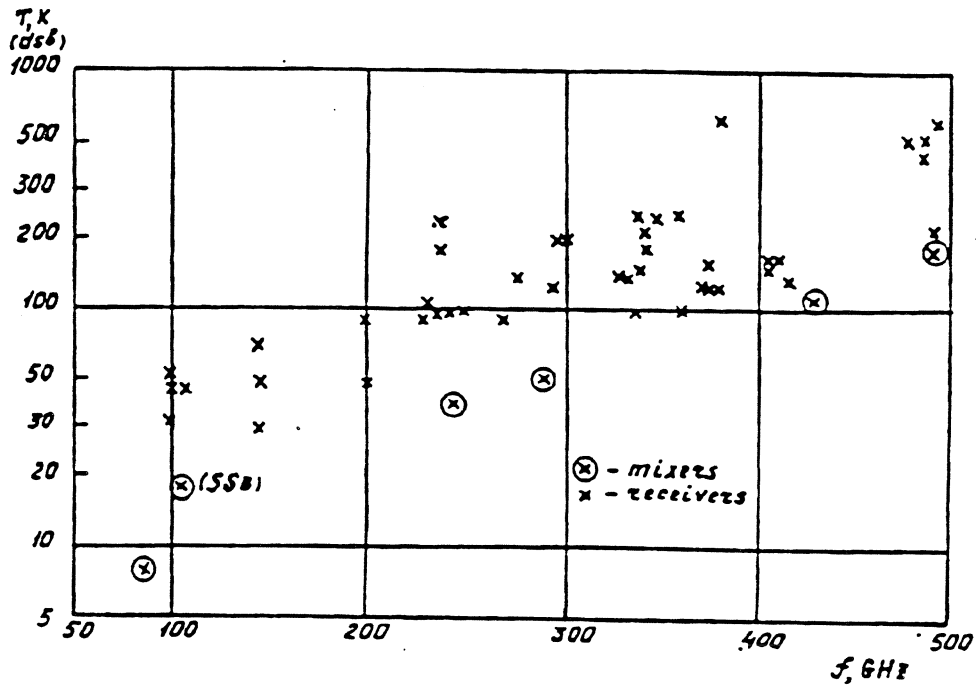


Figure 1. SIS receivers and mixers DSB noise temperatures in 50-500 GHz frequency band.

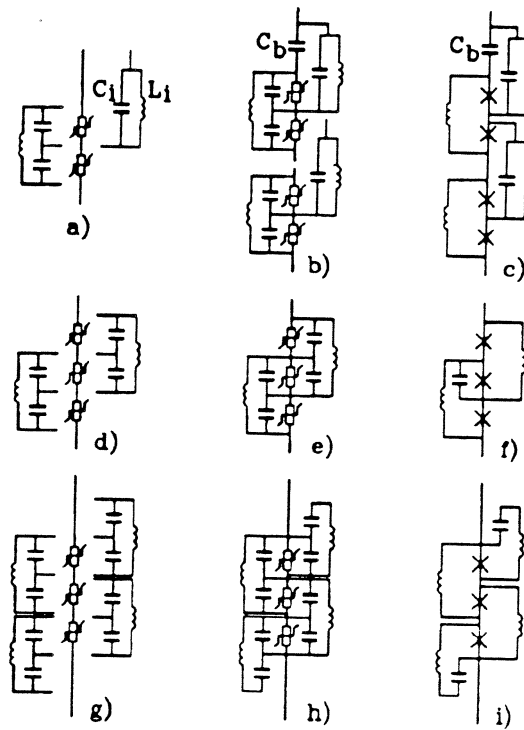


Figure 2. The illustration for the design principle developed for the parallel biased arrays: a)-c) for even number of junctions; d)-f) and g)-i) for odd number of junctions in the array.

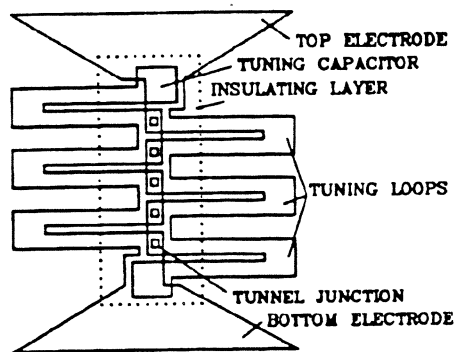


Figure 3. The layout of experimental 5-junctions array as an example of practical realization of variant i) from Figure 1.

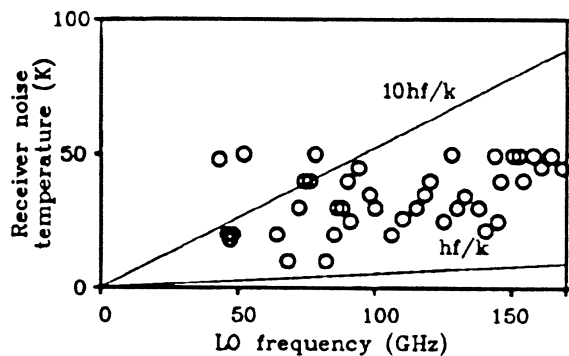


Figure 4 The summary for our best receivers tested in 40-150 GHz frequency range in comparison with quantum limit  $hf/k$ .

150

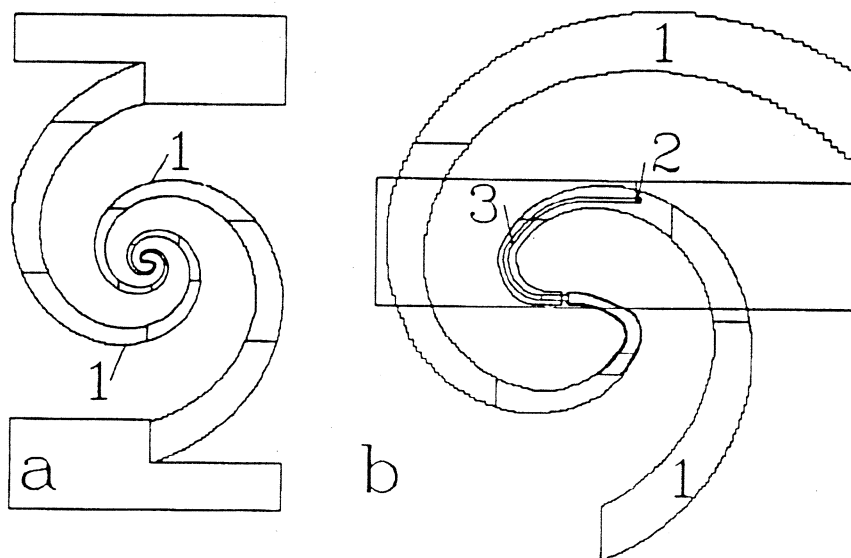


Figure 5. Quasioptical receiver structure for 115 GHz (left) and magnified central part (right) 1 - spiral antenna, 2 - VIA SIS, 3 - microstrip transformer.



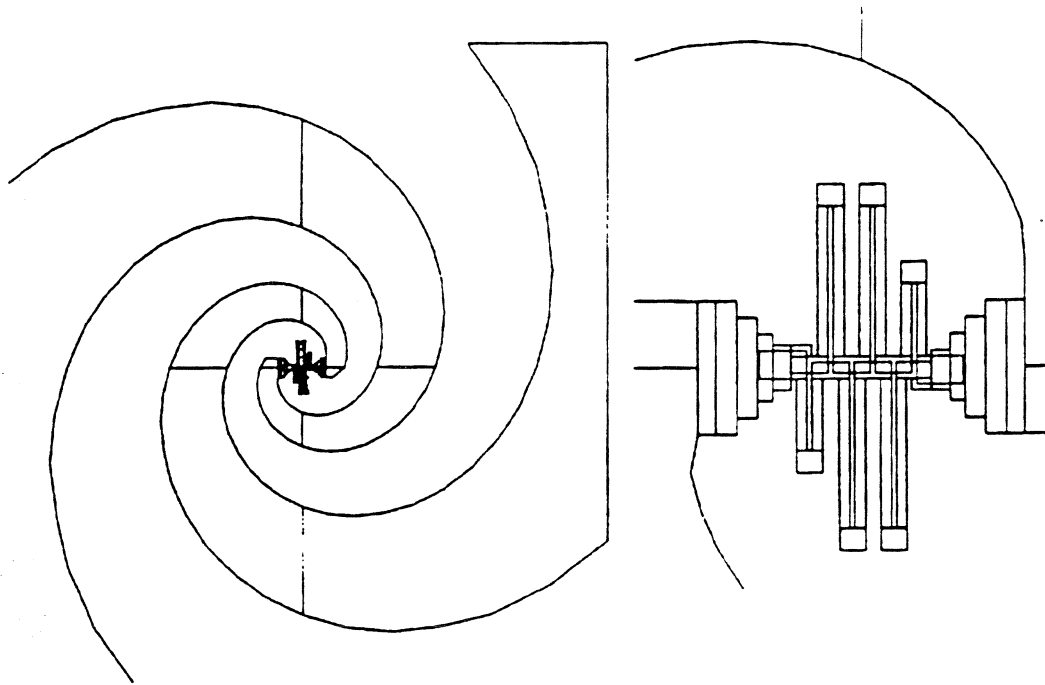


Figure 6. a) Self-babinet spiral antenna  
 b) Series-parallel array consisting of five SIS junctions  $1.5 \mu\text{m}^2$  area each, six inductive short-ended slot lines and two decoupling capacitances.

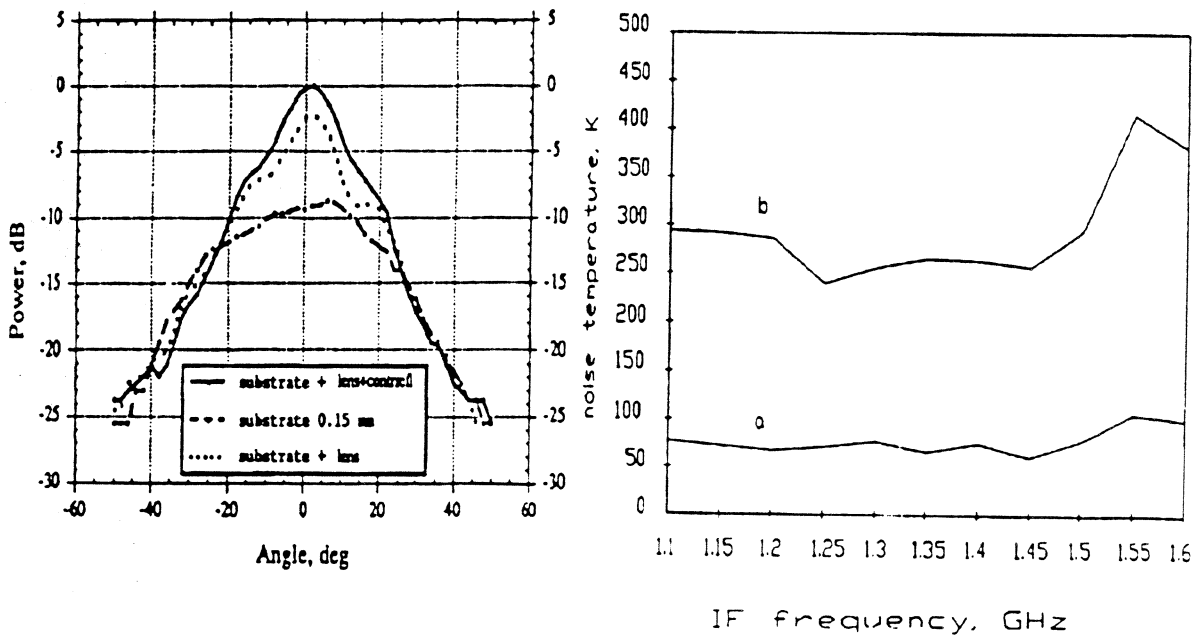
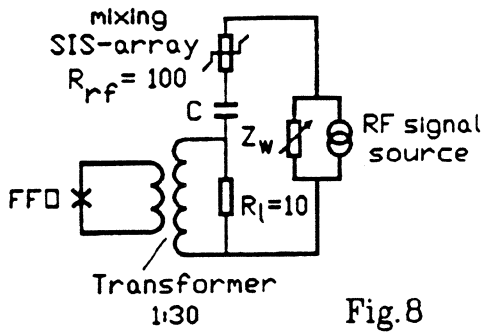
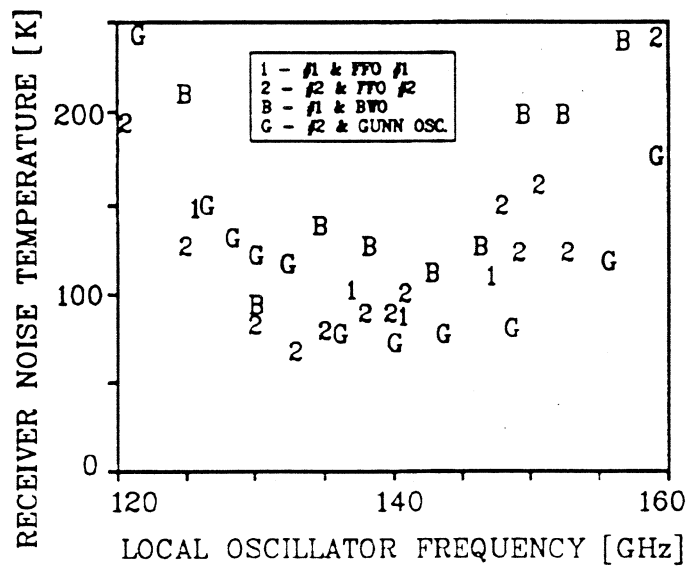
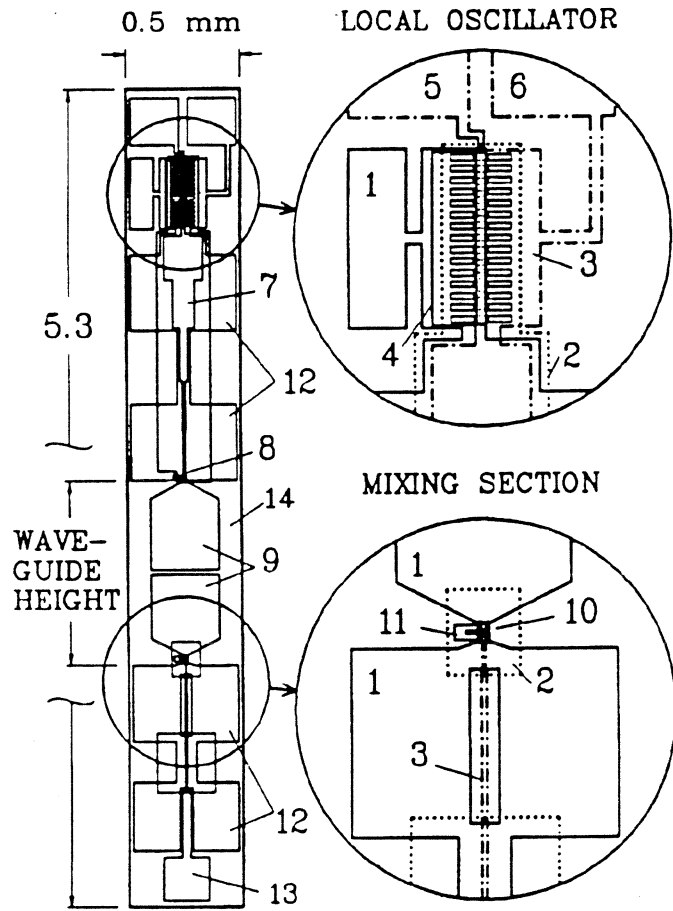


Figure 7. a) Beam patterns of spiral antenna on quartz substrate, the same on quartz hyperhemisphere lens and with counterreflector.  
 b) Noise temperature for closed (a) and opened (b) 8.8 db cold attenuator



1. BOTTOM ELECTRODE (Nb)
2. INSULATION (SiO)
3. TOP ELECTRODE (Nb)
4. DAMPING RESISTOR (Ti)
5. NONUNIFORM FEED PAD
6. UNIFORM FEED PAD
7. MICROSTRIP TRANSFORMER
8. OSCILLATOR LOAD
9. COUPLING PROBES
10. SIS ARRAY
11. INDUCTIVE TUNER
12. RF LOW-PASS FILTERS
13. IF OUTPUT AND BIAS PAD
14. QUARTZ SUBSTRATE



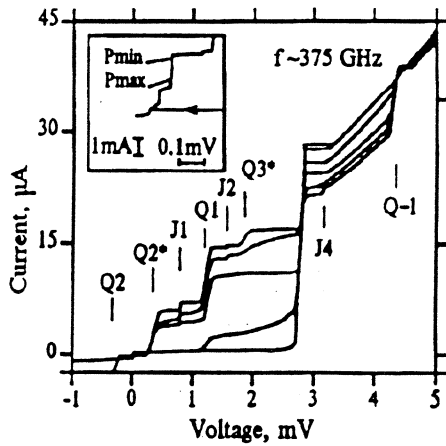


Figure 11. IVC of the detector at different levels of the FFO power adjusted by tuning the bias current at constant magnetic field.

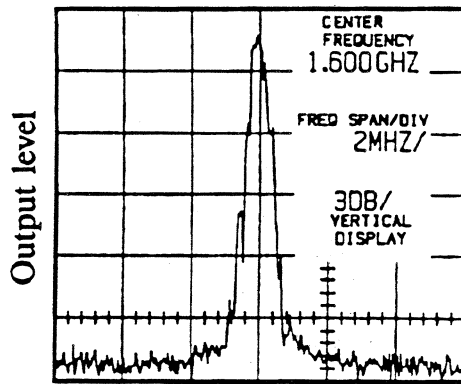


Figure 12. Spectrum of the IF output power when the signal of FFO is mixed with synchronized signal in SIS mixer at 140 GHz.

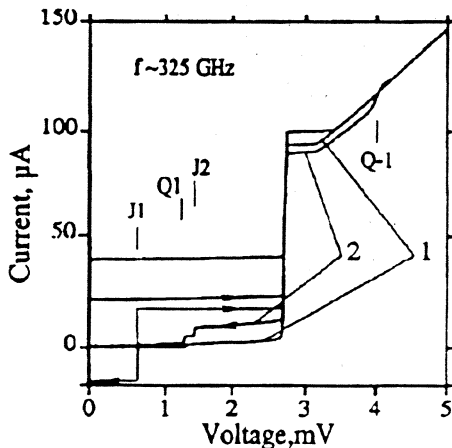


Figure 13. IVC of SIS detector at two levels of the FFO power ( $f=325$  GHz); adjustable attenuation is introduced by superconducting attenuator.

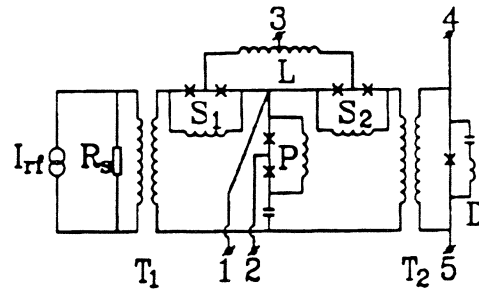


Figure 14. Equivalent diagram of the integrated attenuator circuit.

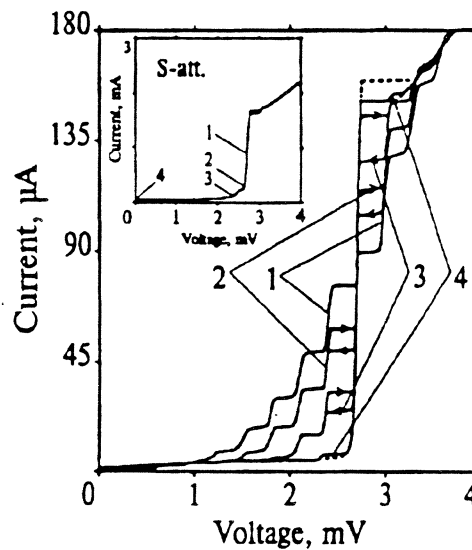


Figure 15. IVCs of the detector at four different bias voltages on the series attenuator for constant level of the input power  $f=74.6$  GHz. IVC of S-att is shown in the insertion.

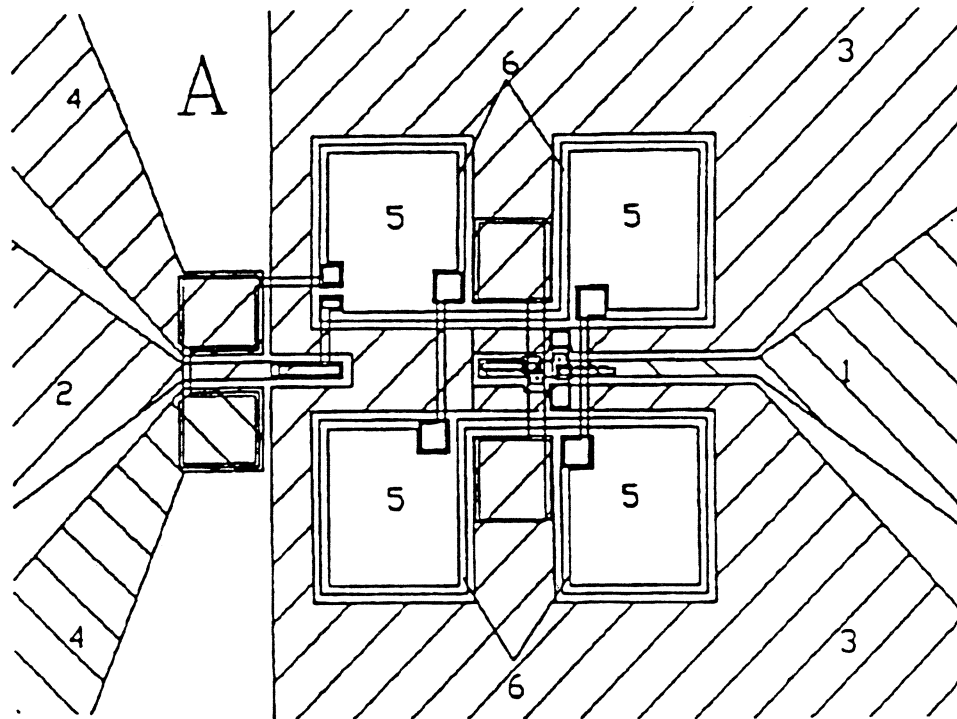


Figure 16. Four-loop planar dc SQUID with integrated input coil. (1,3) and (2,4) - output and input coplanar lines. (5) - parallel connected inductive SQUID loops each  $200 \times 200 \text{ mm}^2$ , inside each of them single turns are arranged and connected in series to form an input coil.

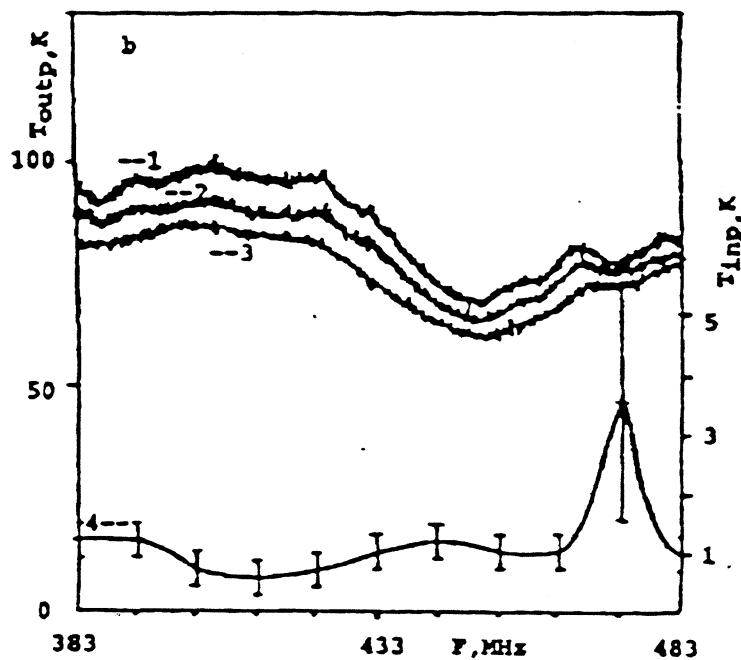


Figure 17. The dependence of the amplified noise signal on frequency. The noise temperature is lower than  $0.5 \text{ K}$  in  $60 \text{ MHz}$  band